American Mineralogist, Volume 75, pages 859–873, 1990

Fluorian garnets from the host rocks of the Skaergaard intrusion: Implications for metamorphic fluid composition

CRAIG E. MANNING,* DENNIS K. BIRD
Department of Geology, Stanford University, Stanford, California 94305, U.S.A.

ABSTRACT

Zoned, silica-deficient, calcic garnets containing up to 5 mol% F substitution for O formed during contact metamorphism of basalts by the Skaergaard intrusion in East Greenland. Fluorian calcic garnets occur as a retrograde alteration of prograde wollastonite and clinopyroxene that fills vesicles and vugs in lavas 30–70 m from the intrusion. Paragenetically equivalent phases include fluorite, wollastonite, calcic clinopyroxene, prehnite, quartz, and calcite. Electron microprobe analysis shows that the garnets are ≥93 mol% grossular-andradite (grandite) solid solutions and that the F content does not fully compensate for the silica deficiency, suggesting the presence of a hydrous component in the garnets. The garnets display discontinuous zoning with respect to Al and Fe, and increases in F, calculated OH, and the Si deficiency with increasing Al concentration are observed. The garnets formed at temperatures between 200 and 420 °C based on the coexisting mineral assemblage, and stratigraphic reconstructions indicate pressures of ~1 kbar.

Assessment of isobaric, isothermal phase relations in the system CaO-Al_2O_3-SiO_2-H_2O-HF allows estimation of fluid characteristics in equilibrium with fluorian grandite-bearing assemblages. The presence of fluorite, wollastonite, quartz, and calcite with these garnets combined with fluid inclusion data require that the activity (a) of H_2O was ~1 and that $a_{H^+}a_{F^-}$ was $10^{-10.5}$ to $10^{-10.0}$ in the coexisting hydrothermal solutions at 200–420 °C and 1 kbar. If pH was neutral at these pressure and temperature conditions (5.3 ± 0.1), the value of a_{F^-} associated with fluorian garnet formation was $10^{-4.7}$ to $10^{-5.2}$. The F content of garnet is extremely sensitive to minor changes in fluid composition. The calculations show that a decrease in pH or an increase in log a_{F^-} of 0.3 at constant pressure and temperature will decrease the F concentration in garnet from 5 to 0 mol%. The results of this study show that fluorian hydrous grandites provide a mineralogical record of the activities of F species in coexisting metamorphic and hydrothermal fluids.

INTRODUCTION

The concentrations of F and OH in minerals such as micas and apatites have been used to infer activities of F species in coexisting fluids (e.g., Eugster and Wones, 1962; Munoz and Ludington, 1974, 1977; Korzhinskii, 1981; Munoz, 1984). In grossular-andradite (grandite) solid solutions, the substitution of OH is well documented (e.g., Pabst, 1942; Peters, 1965; Cohen-Addad et al., 1967; Lager et al., 1987, 1989), and the recent recognition of F substitution suggests that this phase can also be used to constrain activities of F species in geologic fluids. Grandite garnets with up to 3.6 wt% F have been reported from three geologic environments. These environments include metamorphosed and metasomatically altered carbonates (Dobson, 1982; Yun and Einaudi, 1982; Valley et al., 1983), metasomatically altered alkaline intrusive rocks (Nash and Wilkinson, 1970; Flohr and Ross, 1989), and contact-metamorphosed basalts (van Marcke de Lummen, 1986). Even higher F concentrations (up to 5.6 wt%) have been observed in subcalcic Mn-rich garnets from the porphyry Mo deposit at Henderson, Colorado (Smyth et al., 1990; Seedorff, 1987).

Cell-edge refinements of natural fluorian garnets indicate that F replaces O in the garnet structure (Valley et al., 1983; Smyth et al., 1990). To account for the observed F enrichment in grossular-rich fluorian garnets, Valley et al. (1983) suggested that F may enter the garnet lattice via two coupled substitutions:

$$[^{[4]}\square(OH,F)_4]^{4-} = [^{[4]}SiO_4]^{4-} \quad (1)$$

and

$$[^{[6]}M^{2+}(OH,F)]^{+} = [^{[6]}M^{3+}O]^{+}, \quad (2)$$

where the superscripts [4] and [6] denote tetrahedrally and octahedrally coordinated sites, □ represents a vacancy in the designated site, and M denotes a cation with the superscripted charge. In grandite garnets with low $^{[6]}M^{2+}$ contents, most F and OH will be accommodated by Equation 1. Because Equation 1 involves exchange of Si,

* Present address: U.S. Geological Survey, M.S. 910, 345 Middlefield Rd., Menlo Park, California 94025, U.S.A.

0003–004X/90/0708–0859$02.00

O, F, and H, the extent of substitution and zoning in F- and OH-bearing grandites may be used to evaluate relative changes in the chemical potentials of the thermodynamic components H_2O, HF and SiO_2 in coexisting metamorphic and hydrothermal fluids.

In this paper we report new analyses of F-bearing garnets from the contact-metamorphosed basaltic country rocks of the Skaergaard intrusion, East Greenland. We use natural phase equilibria to derive a method for using the F content of grandite garnets to evaluate the chemical potential of the HF in the coexisting fluid phase. These methods are used to compare the East Greenland garnets to F-bearing grandites from the Adirondacks to evaluate differences in metamorphic fluid compositions between the environments.

Occurrence

Heat transfer associated with the emplacement and cooling of the gabbroic Skaergaard intrusion (Fig. 1) caused hydrothermal fluid circulation and metamorphism in its host rocks (Wager and Deer, 1939; Taylor and Forester, 1979; Norton and Taylor, 1979; Norton et al., 1984; Bird et al., 1985, 1986, 1988a, 1988b; Manning, 1989; Manning and Bird, 1986, in preparation). Interbedded basaltic aa and vesicular lavas (Fig. 2) were metamorphosed during crystallization and cooling of the gabbro. The map area in Figure 2 can be divided into three metamorphic mineral zones: the actinolite + chlorite zone (>210 m from the contact), the pyroxene zone (10–210 m), and the olivine zone (0–10 m). Diagnostic minerals include metamorphic olivine in the olivine zone, metamorphic clinopyroxene and orthopyroxene in the pyroxene zone, and actinolite and chlorite replacing magmatic clinopyroxene in the actinolite + chlorite zone. Peak metamorphic temperatures ranged from ~1000 °C at the contact to ~300 °C at 500 m. Lithostatic pressure was ~1 kbar as estimated from a burial depth of 4 ± 1 km (Manning, 1989).

After the development of prograde metamorphic mineral assemblages, the contact aureole was crosscut by a series of vertical veins associated with mafic dike emplacement and the cooling and contraction of the solidified gabbro and its host rocks. Based on fracture-filling mineral assemblages and textures, the veins can be divided into two types: (1) granophyres with granophyric intergrowths of quartz and potassium feldspar that probably reflect crystallization from a silicate liquid, and (2) veins filled by hydrothermal mineral assemblages, including actinolite + chlorite, epidote + quartz, and quartz. The granophyres formed shortly after gabbro crystallization and occur within 100 m from the intrusive contact. Hydrothermal veins cross cut the granophyres and are found throughout the area shown in Figure 2 (Manning, 1989).

Fluorine-bearing garnets are associated with complex calc-silicate mineral assemblages in paleo-pore structures (amygdules) <5 cm wide that include breccia matrices and vesicles. Amygdules containing fluorian grandites occur in a restricted area of the pyroxene zone between 30 and 70 m from the contact (Fig. 2). Petrographic examination of six garnet-bearing samples from this zone (Fig. 2) allows division of the pore-filling minerals into early and late assemblages based on overgrowth and replacement textures. The early assemblage at the margins of the amygdules consists of ferroan diopside to magnesian hedenbergite, with minor apatite and titanite, whereas the early assemblage in amygdule centers consists of prismatic wollastonite and magnesian hedenbergite.

Fluorine-bearing garnets formed as part of a later, retrograde assemblage altering prismatic wollastonite and pyroxene in amygdule centers. Other retrograde minerals in amygdule centers are fluorite, calcite, quartz, acicular wollastonite, and magnesian hedenbergite. Near the walls of amygdules, prehnite and locally calcite overgrow early pyroxene, apatite, and titanite. Prehnite and calcite are paragenetically equivalent to the late garnet-bearing assemblage found in amygdule centers.

The garnets are up to 0.5 mm in the longest dimension, range from subhedral to anhedral crystal forms, and are zoned (Fig. 3). Figure 3 shows that garnet cores have high backscattered electron intensities, and qualitative energy dispersive analysis indicates that these zones are Fe-rich. All garnets display discontinuous outward zoning to more Al-rich compositions with lower intensities of backscattered electrons (e.g., point labeled "b" in Fig. 3A). Zoning in the garnets is also marked by abrupt reversals in composition; for example, the point labeled "c" in Figure 3A is more Fe-rich than earlier formed compositions.

The hydrothermal fluids associated with mineralogic and isotopic alteration of the Skaergaard's basaltic host rocks were dilute meteoric waters with ~1.5 wt% NaCl equivalent (Taylor and Forester, 1979; Bird et al., 1988b; Manning, 1989) and probably did not contain substantial F. However, the later alteration assemblage containing F-bearing minerals such as fluorite and fluorian garnet occurs only in the portion of the aureole <100 m from the contact where granophyre veins are found (Manning and Bird, in preparation). Bird et al. (1986) report fluid inclusions with ~8 wt% NaCl equivalent in quartz from these granophyres. It therefore seems likely that the fluorine-bearing minerals formed as a consequence of local mixing of dilute aqueous pore fluids and fluids exsolved from the granophyres.

Analytical methods

Garnet compositions were determined using a JEOL 733A electron microprobe with five wavelength-dispersive spectrometers. Operating conditions included 15 kV accelerating potential, 15 nA current on Faraday cup, a defocused 5–10 μm beam diameter, and counting times of 40 s for F and 30 s for all other elements. Weight fractions of oxides were calculated using a Bence and Albee (1968) matrix correction scheme (Chambers, 1985). Compositional uncertainties given in this study reflect random errors in X-ray counts and were calculated from the product of the k-ratio, the correction factor used to

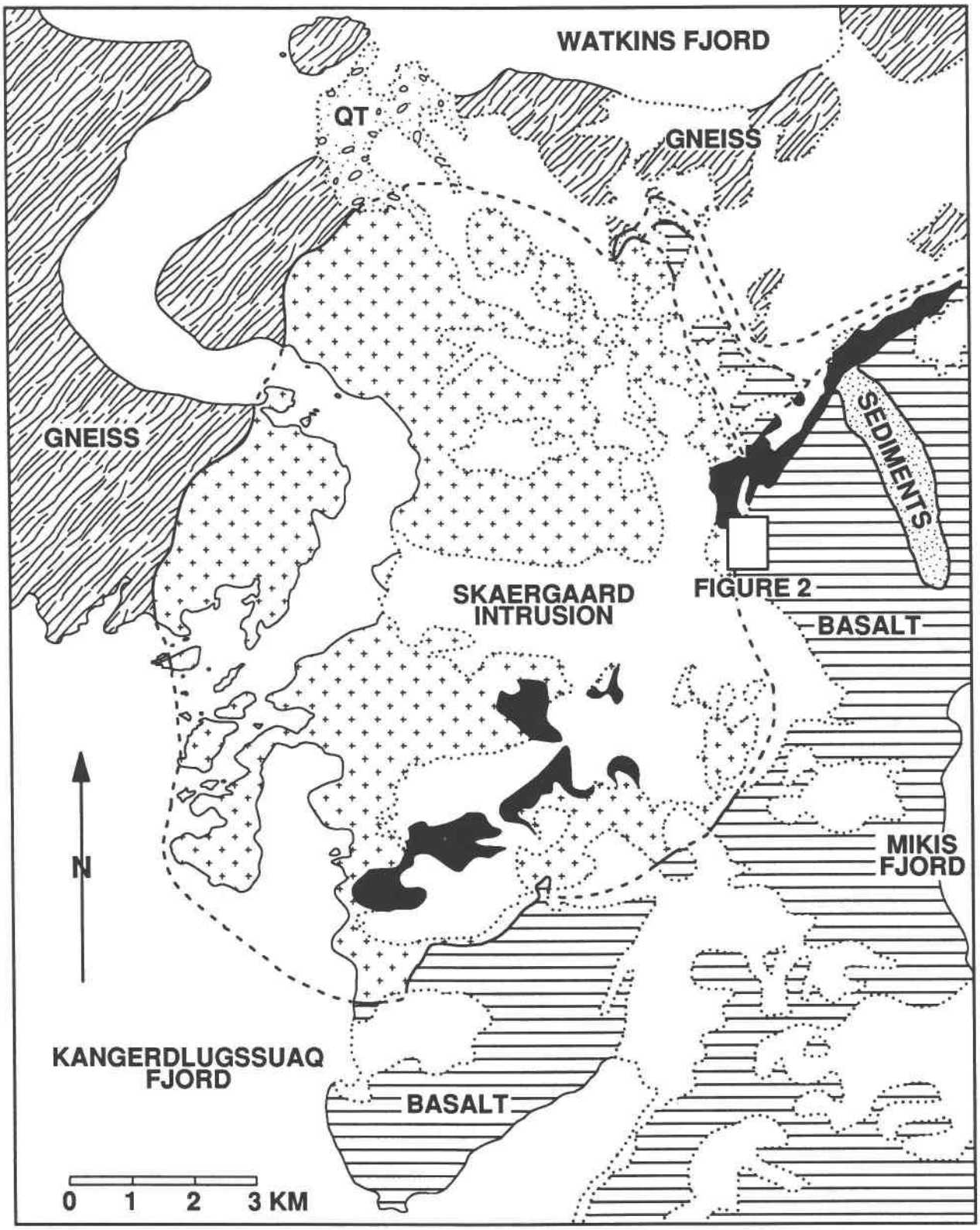

Fig. 1. Geologic map showing the Skaergaard intrusion and its host rocks (modified after Bird et al., 1986).

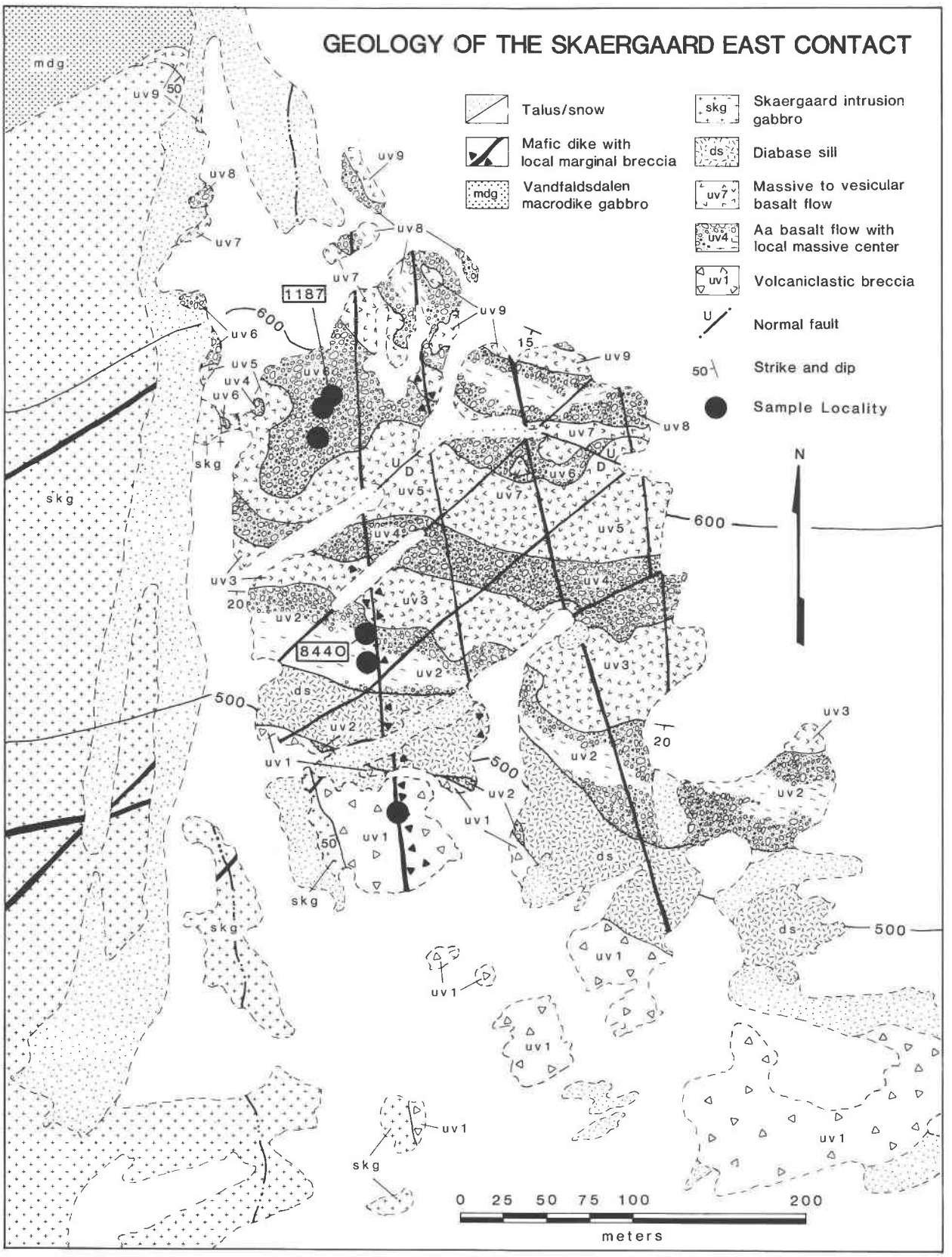
GEOLOGY OF THE SKAERGAARD EAST CONTACT
Talus/snow
Mafic dike with local marginal breccia
mdg Vandfaldsdalen macrodike gabbro
skg Skaergaard intrusion gabbro
ds Diabase sill
uv7 Massive to vesicular basalt flow
uv4 Aa basalt flow with local massive center
uv1 Volcaniclastic breccia
Normal fault
Strike and dip
Sample Locality
N
1187
8440
600
500
0 25 50 75 100 200
meters

TABLE 1. Comparison of analyses of a single garnet zone using different F standards

	Average analysis using fluorian topaz as F standard (5 analyses)	Average analysis using fluorian phlogopite as F standard (4 analyses)	Uncertainty*
	Weight percent		
SiO_2	34.29	34.09	0.17
TiO_2	<0.02	<0.02	0.02
Al_2O_3	20.89	20.69	0.13
Fe_2O_3**	2.72	2.78	0.07
MnO	0.86	0.82	0.04
MgO	<0.04	<0.04	0.01
CaO	36.07	35.86	0.23
F	2.56	2.64	0.32
Sum	97.39	95.77	
$-F \equiv O$	−1.08	−1.11	
	96.31	95.77	
H_2O†	3.97	3.82	0.29
	100.28	99.59	
	Atoms per 5 (X + Y) atoms		
Si	2.596	2.598	0.006
$^{[4]}\square$	0.404	0.402	0.006
Ti	<0.001	<0.001	0.001
Al	1.864	1.859	0.008
Fe^{3+}	0.136	0.140	0.004
Fe^{2+}	0.019	0.019	0.004
Mn	0.055	0.053	0.003
Mg	<0.005	<0.005	0.005
Ca	2.926	2.928	0.008
F	0.613	0.636	0.068
OH‡	1.003	0.972	0.074

* Uncertainties apply to both analyses and reflect random errors in X-ray counts (see text).

** All Fe as Fe_2O_3.

† H_2O weight fraction converted from OH calculated by Equation 3 (see text).

‡ Calculated by Equation 3 (see text).

convert the k-ratio to weight percent, and one standard deviation in the k-ratio (Chambers, 1985).

Fluorine was analyzed using a TAP crystal with a stretched 100 Å polypropylene spectrometer window mounted on Ni mesh. The F minimum detection limit was 0.10 wt% under the operating conditions given above and the maximum observed F peak-to-background ratio was 9.8. Fluorian topaz (Barton et al., 1982) was used as the F standard for all analyses reported here; however, Solberg (1982) and Valley (personal communication, 1989) have observed that topaz F Kα peak shapes differ from those for micas, amphiboles, apatites, and fluorides, and these workers suggest that this can lead to errors of ~20% in F concentration. To evaluate possible systematic errors owing to the choice of standard, we reanalyzed a single F-rich portion of a garnet from sample 1187 using as F standards both fluorian topaz (20.3 wt% F) and

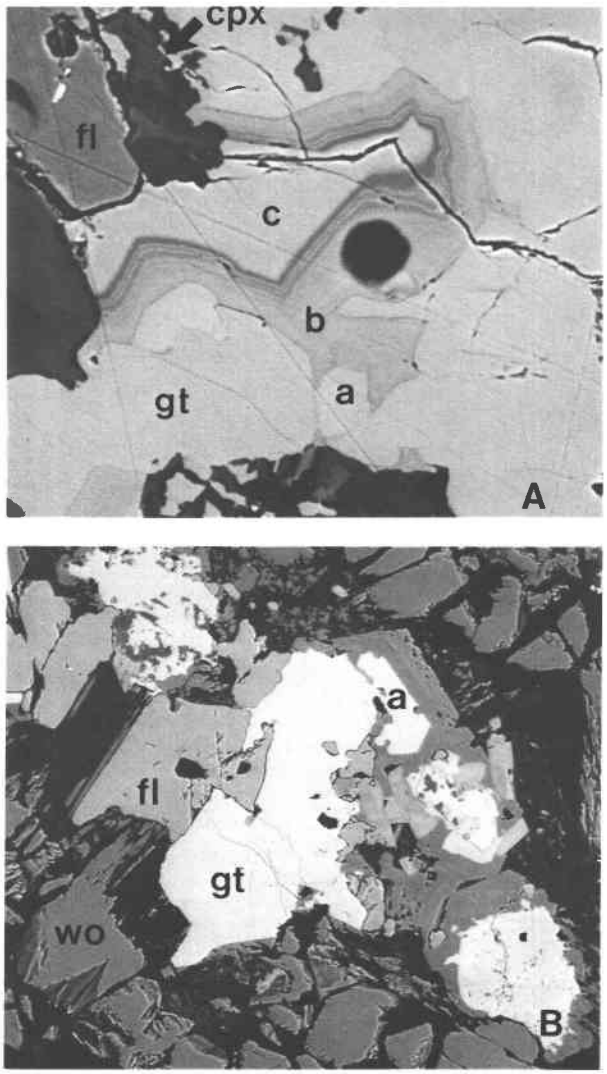

Fig. 3. Backscattered electron images of zoned F-bearing grandite garnets from the east contact of the Skaergaard intrusion. High and low intensity signatures correspond to iron- and aluminum-rich zones, respectively. (**A**) Anhedral garnet (gt) coexisting with clinopyroxene (cpx) and fluorite (fl) in sample 844O. The earliest garnet grains (a) are Fe-rich, the intermediate portions (b) show discontinuous, oscillatory zoning alternating between Al- and Fe-rich compositions, and the latest garnet (c) is Fe-rich. Field of view is 120 μm wide. (**B**) Subhedral, discontinuously zoned garnet coexisting with wollastonite (wo) and fluorite in 844O. Note well-developed crystal faces and sharp compositional breaks at (a). Field of view is 400 μm wide.

←

Fig. 2. Geology of the Skaergaard east contact. The elevation contours are in meters above sea level, and the labels uv1–uv10 denote individual lava flows in the map area. Localities at which fluorian grandites have been found are shown with the filled circles and samples 844O and 1187 are discussed in the text.

TABLE 2. Representative garnet analyses

Sample	8440						1187			
analysis	d3 core	d14 int*	d1 rim	h1 core	h2 rim	i4 rim	c1 core	c4 int*	c8 int*	c7 rim
	Weight percent									
SiO_2	34.87	33.76	34.22	34.21	36.24	31.20	33.69	35.00	35.41	33.89
TiO_2	0.05	<0.02	<0.02	<0.02	0.32	0.33	<0.02	0.62	1.57	0.03
Al_2O_3	0.35	9.48	0.16	<0.05	17.29	15.62	<0.05	2.17	9.70	20.93
Fe_2O_3**	30.64	17.97	30.56	31.03	7.03	8.82	31.55	27.57	16.05	2.80
MnO	1.57	0.19	0.07	<0.04	0.37	0.29	0.57	0.11	0.15	0.97
MgO	0.07	0.16	0.44	0.14	<0.04	<0.04	0.14	0.07	0.09	<0.04
CaO	31.55	35.34	32.67	32.94	36.39	35.79	32.20	33.22	34.69	35.94
F	<0.10	0.91	0.33	<0.10	1.47	1.56	<0.10	0.38	0.19	2.70
Cl	<0.02	<0.02	<0.02	<0.02	<0.02	<0.02	<0.02	<0.02	<0.02	<0.02
H_2O†	0.45	4.03	1.14	1.30	2.09	7.08	2.01	0.53	2.06	4.39
Sum‡	99.55	101.46	99.45	99.62	100.58	100.04	100.16	99.51	99.82	100.51
	Atoms per 5 (X + Y) atoms									
Si	2.968	2.680	2.904	2.906	2.777	2.441	2.858	2.938	2.850	2.562
$^{[4]}\square$	0.032	0.320	0.096	0.094	0.223	0.559	0.142	0.062	0.150	0.438
Ti	0.003	<0.001	<0.001	<0.001	0.018	0.019	<0.001	0.039	0.095	0.002
Al	0.035	0.887	0.016	<0.005	1.562	1.441	<0.005	0.215	0.920	1.865
Fe^{3+}	1.950	1.074	1.952	1.983	0.388	0.500	1.981	1.707	0.888	0.130
Fe^{2+}§	0.013	0.000	0.000	0.000	0.017	0.019	0.033	0.035	0.084	0.029
Mn	0.113	0.013	0.005	<0.003	0.024	0.019	0.041	0.008	0.010	0.062
Mg	0.009	0.019	0.056	0.018	<0.005	<0.005	0.018	0.009	0.011	<0.005
Ca	2.877	3.006	2.971	2.998	2.988	3.001	2.926	2.988	2.992	2.911
Sum	8.000	7.999	8.000	7.999	7.999	7.999	7.999	8.001	8.000	7.999
F	<0.027	0.228	0.089	<0.027	0.356	0.386	<0.027	0.101	0.048	0.645
Cl	<0.003	<0.003	<0.003	<0.003	<0.003	<0.003	<0.003	<0.003	<0.003	<0.003
OH‖	0.127	1.066	0.324	0.368	0.534	1.848	0.570	0.148	0.552	1.107

* Intermediate between core and rim.
** All Fe as Fe_2O_3.
† H_2O weight fraction converted from OH calculated by Equation 3 (see text).
‡ Adjusted for O ≡ F.
§ Calculated by charge balance.
‖ Calculated by Equation 3 (see text).

synthetic fluorian phlogopite (9.01 wt% F, synthesized by D. Wones and provided by G. Czamanske). Table 1 gives analyses of the same garnet zone using the different F standards and shows that concentrations of all analyzed elements, including F, are the same within the stated uncertainties.

Calculation of formulae of F- and OH-bearing garnets from electron microprobe analyses is problematic owing to the presence of tetrahedral vacancies, the possibility of tetrahedral coordination of Al, Fe^{3+}, and Ti (Meagher, 1980; Deer et al., 1982, and references therein), and uncertainties in the relative amounts of Fe^{2+} and Fe^{3+}. Valley et al. (1983) normalized garnet formulae to 5 dodecahedral (X) and octahedral (Y) cations and assumed no tetrahedrally coordinated Al, Fe^{3+}, or Ti. Flohr and Ross (1989) calculated formulae based on 12 anions, allowing for tetrahedral coordination of Al, Fe^{3+}, and Ti but assuming that H_2O concentration is equal to 100 minus the oxide sum corrected for other anions. Although substitution of Al, Fe^{3+}, and Ti for Si is common in Ti-rich garnets (e.g., Huggins et al., 1977), the amount of tetrahedral coordination of these cations is small in low-temperature OH-bearing garnets in the presence of quartz (e.g., Huckenholz and Fehr, 1982). Because these conditions obtained during the formation of the garnets discussed here, formulae were normalized to 5 (X + Y) cations as described by Valley et al. (1983). This method yields a minimum estimate of OH concentration through the equation

$$n_{OH} = 4n_{(^{[4]}\square)} - n_F + n_{Ti} - n_{(^{[6]}Mg)} \quad (3)$$

where n is the number of atoms of the subscripted element or vacancy per 5 (X + Y) atoms and $^{[4]}\square$ represents tetrahedral vacancies, which are equal to the difference between n_{Si} and 3.0. The assumption that OH balances charge is supported by infrared absorption spectroscopy, nuclear magnetic resonance spectroscopy, and neutron diffraction studies on natural and synthetic hydrograndites (Cohen-Addad et al., 1967; Lager et al., 1987, 1989). Although additional OH in excess of that calculated from Equation 3 is unlikely (Lager et al., 1989), the lack of a direct determination of Fe_2O_3 and FeO requires that the calculated OH concentration be considered a minimum.

The greatest uncertainty in garnet compositions is the OH content. Inspection of Equation 3 shows that the uncertainty in computed OH can be calculated as the sum of random errors in Mg, Ti, F, and tetrahedral vacancies, where the latter are equivalent to errors in Si concentra-

tion. The relatively large errors in F and Si (Table 1) thus lead to uncertainties of 7.5% in the minimum calculated OH per 5 (X + Y) cations. Such large uncertainties, combined with the possibility of additional OH through Equation 2, indicate that caution should be used in interpreting OH concentrations computed by charge balance.

Garnet compositions

Representative compositions of fluorian garnets from samples 844O and 1187 (Fig. 2) are in Table 2. Garnets from these samples are ≥93% grossular-andradite solid solutions and range in mole fraction of aluminum [X_{Al}, where $X_{Al} = n_{Al}/(n_{Al} + n_{Fe^{3+}})$] from 0.00 to 0.93. Maximum observed pyralspite components are 0.8% $Mg_3Al_2Si_3O_{12}$, 3.7% $Mn_3Al_2Si_3O_{12}$, and 1.1% $Fe_3Al_2Si_3O_{12}$. Garnets are melanitic between cores and rims in sample 1187 and contain between 0.039 and 0.168 Ti atoms per 5 (X + Y) atoms (2.0–8.4% Ti in Y). All other garnets contain <0.5 mol% Ti. Chlorine is below detection limit (0.02 wt%) in all garnets analyzed.

In Figure 4A the F contents of calcic garnets are shown as a function of X_{Al}, and it can be seen that F concentration increases with increasing grossular component. The positive correlation between F and X_{Al} suggests that the substitution of F into garnet will be favored by bulk compositions poor in Fe^{3+}. Figure 4B illustrates that X_{Si} ($X_{Si} = n_{Si}/3$) decreases with increasing grossular content. All garnet compositions in this study have $X_{Si} < 1.0$ and are therefore silica-deficient. Iron-rich zones are closest to full Si occupancy (n_{Si} = 2.80–2.96), and the maximum silica deficiency in Al-rich zones is 21%. The Si deficiency is greater than $4n_F$ in all analyzed garnets, suggesting the presence of OH (Eq. 3). Minimum OH concentrations calculated from Equation 3 are 0.1 to 0.9 ± 0.1 at $X_{Al} < 0.1$ and 0.5 to 2.2 ± 0.1 at $X_{Al} > 0.8$. The relationship between F and calculated OH, as expressed by $n_F/(n_F + n_{OH})$, is given in Figure 4C. Although there is a wide scatter in the data, Figure 4C shows that $n_F/(n_F + n_{OH}) < 0.5$ in all analyzed garnets. Note that since computed OH is a minimum value, $n_F/(n_F + n_{OH})$ shown in Figure 4C is a maximum.

Temperature of garnet formation

The temperature of garnet formation can be estimated from the mineral assemblage coexisting with F-bearing garnets. The formation of prehnite during retrograde alteration constrains maximum temperatures of the garnet-bearing assemblage to 420 °C at the 1-kbar pressure of contact metamorphism, based on univariant equilibrium among stoichiometric prehnite, grossular, zoisite, quartz, and H_2O (Liou, 1971; Connolly and Kerrick, 1985) using the data of Helgeson et al. (1978). This is a maximum estimate because substitution of Fe^{3+} and OH in garnet and Fe^{3+} in prehnite and epidote solid solutions will decrease the temperature of this equilibrium at constant pressure (Bird and Helgeson, 1980; Rose and Bird, 1987).

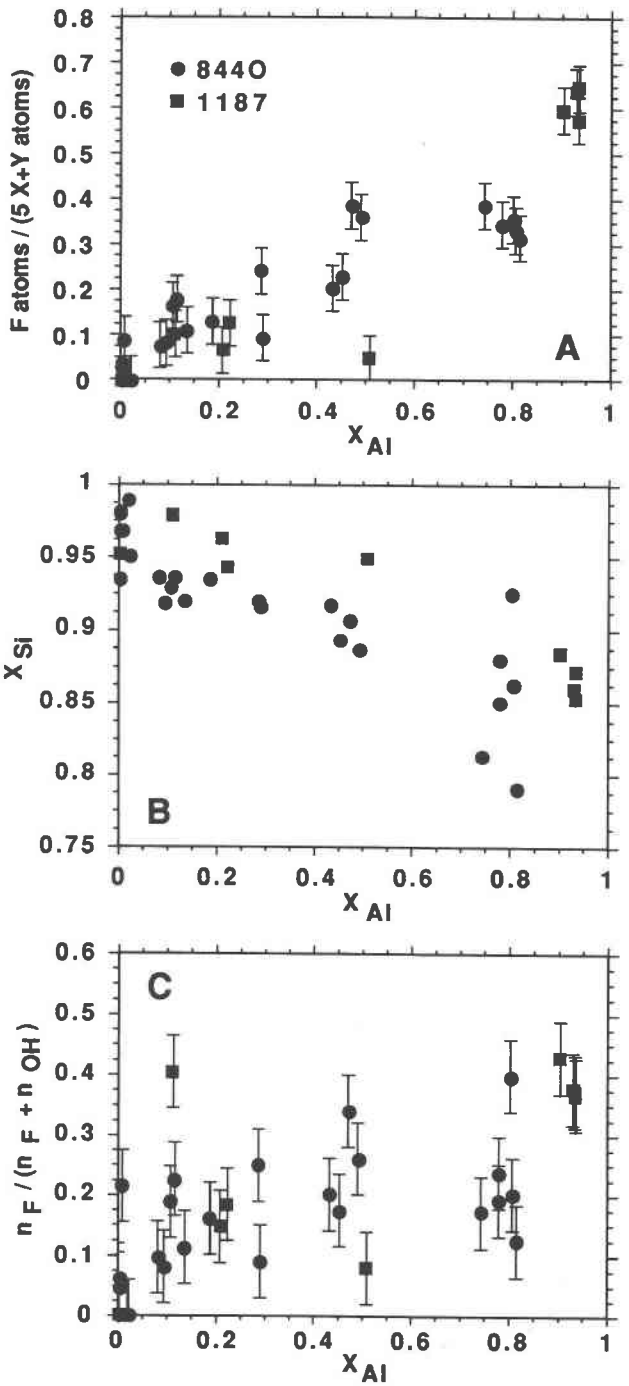

Fig. 4. Compositional parameters as a function of mole fraction of octahedral aluminum [X_{Al}, where $X_{Al} = n_{Al}/(n_{Al} + n_{Fe^{3+}})$] in calcic garnets: (**A**) F atoms per 5 (X + Y) atoms, (**B**) mole fraction of Si (X_{Si}, where $X_{Si} = n_{Si}/3$), and (**C**) $n_F/(n_F + n_{OH})$. Uncertainties are calculated from random errors in X-ray counts (see text) and are shown only when larger than the symbols used.

The absence of xonotlite in the alteration assemblage provides an approximate lower temperature limit of 200–275 °C, as deduced from the unreversed 1-kbar dehydration of xonotlite to wollastonite (Gustafson, 1974). Thus the garnets probably formed between 200 and 420 °C.

The unreversed experimental data of Huckenholz and Fehr (1982) suggest that there is a compositional gap in hydrous grandite solid solutions with a critical temperature of 450–500 °C and a critical composition of $X_{Al} \sim 0.55$. Inspection of Figure 4 shows that no analyses occur between $X_{Al} = 0.50$ and $X_{Al} = 0.75$, implying that the natural samples exhibit a compositional gap that is consistent with the experimental observations of Huckenholz and Fehr (1982). If it exists, a solvus in hydrous grandite would be an excellent thermometer for low-grade metabasalts and calc-silicates; but estimation of temperatures from the available experimental data is highly uncertain.

Comparison with other fluorian calcic garnets

Fluorine-bearing calcic garnets have been reported in metamorphosed impure carbonates, metasomatically altered alkaline igneous rocks, and contact-metamorphosed basalts. The occurrence, phase relations, and compositional characteristics of fluorian grandite in these environments are compared below.

Occurrence of fluorian grandite

Metacarbonates. In impure carbonates, fluorian calcic garnets are associated with skarn assemblages that developed during prograde contact metamorphism at Lost River, Alaska (Dobson, 1982, 1984) and at Ulchin and Yeonhwa, South Korea (Yun, 1979; Yun and Einaudi, 1982). At Lost River, F-bearing grandite occurs in monomineralic zones that are crosscut by veins containing fluorite, vesuvianite, and magnetite. Fluid inclusion homogenization temperatures suggest conditions of garnet formation were >400 °C (Dobson, 1984). Associated minerals in the South Korean skarns include variable amounts of pyroxene, Mn-pyroxenoid, fluorite, quartz, calcite, biotite, chlorite, hematite, and sulfides (Yun, 1979); however, no temperature estimates for the formation of this assemblage are reported. Fluorine-bearing grandites also formed during retrograde alteration of amphibolite facies marbles in the Adirondack mountains of eastern New York (Valley et al., 1983). Valley et al. (1983) reported fluorian grandites coexisting with quartz, pumpellyite, prehnite, and calcite. The maximum thermal stability of prehnite limits the temperature of Adirondack garnet formation. The univariant equilibrium among prehnite, zoisite, grossular, quartz, and H_2O has a steep negative slope, occurring at 420 °C at 1 kbar and 380 °C at 5 kbar, and maximum temperatures inferred from the presence of prehnite are therefore relatively insensitive to pressure. Thus, although Valley et al. (1983) did not give a pressure estimate for the retrograde alteration, the presence of prehnite in the alteration assemblage requires that the maximum temperature of fluorian-garnet formation in the Adirondacks was 400 ± 20 °C. All F-bearing garnets from metacarbonate lithologies are grossular-andradite solid solutions, with calculated Mn, Mg, and Fe^{2+} concentrations in dodecahedral sites exceeding 10 mol% in only a few of the report analyses. The calcic garnets from Lost River contain 0.7–9.7 mol% Sn (Dobson, 1982, 1984), and Sn content decreases with increasing Al and F.

Alkaline igneous rocks. F-bearing grandite garnets occur as part of metasomatic alteration assemblages in alkaline igneous rocks that include nepheline syenites in the Shonkin Sag laccolith, Montana (Nash and Wilkinson, 1970) and garnet-ijolite xenoliths in nepheline syenite at Magnet Cove, Arkansas (Flohr and Ross, 1989). Fluorian grandites are associated with aegerine augite, biotite, zeolites, and nepheline at both localities. At Shonkin Sag, sanidine and arfvedsonite are part of the primary igneous assemblage, and carbonate occurs with zeolites and garnet as alteration of magmatic nepheline. At Magnet Cove, fluorian garnets occur as secondary overgrowths on magmatic melanite garnets. In addition, apatite, titanite, and magnetite are both primary and secondary phases, and cancrinite occurs with zeolite as alteration of nepheline. All F-bearing garnets from altered alkaline rocks contain >93 mol% Ca in dodecahedral positions, but contain substantial concentrations of octahedral Ti (5.2–10.7 mol%). The F content of garnets reported by Flohr and Ross (1989) decreases with increasing Ti concentration. These garnets also contain minor quantities of Zr, V, Nb, and Na.

Metabasalts. In addition to the occurrence in the metabasalt host rocks of the Skaergaard intrusion described in this paper, F-bearing grandites also occur in basalts that were metamorphosed during emplacement of the Land's End granite in Cornwall, England (van Marcke de Lummen, 1986). At the latter locality, garnets occur in quartz-rich nodules and are interpreted to have formed at ~600 °C (van Marcke de Lummen and Verkaeren, 1985). Coexisting minerals include magnetite, quartz, potassium feldspar, epidote, and apatite. These garnets contain up to 0.27 wt% K_2O, 0.20 wt% ZnO and 0.08 wt% Cl.

Comparison of fluorian grandite compositions

Compositional characteristics of F-bearing grandites from all three environments are in Figure 5. Figure 5A shows that fluorian grandites from metacarbonates and metabasalts display a wide range of Al-Fe^{3+} compositions. Although the five analyses given by Flohr and Ross (1989) suggest a more restricted range in X_{Al} in garnets from alkaline rocks (Fig. 5A), examination of their Figure 7 indicates that there is a continuous range in X_{Al} compositions in Magnet Cove F-bearing grandites from ~0 to 0.64. It can be seen in Figure 5A that in metabasalts and alkaline igneous rocks, there is a decrease in X_{Si} with increasing X_{Al}, indicating greater silica deficiency in more Al-rich garnets. In contrast, X_{Si} in metacarbonates is apparently independent of X_{Al}, and most fluorian grandites from these lithologies have high tetrahedral site occupan-

cy by Si. It is important to note, however, that many garnet compositions reported by Yun (1979) and Yun and Einaudi (1982) have $n_{Si} > 3.02$, suggesting possible systematic errors in their analyses. The degree of F enrichment with increasing X_{Al} in metacarbonates is low relative to that observed in metabasalts and alkaline rocks (Fig. 5B), which is consistent with the higher Si contents of garnets in metacarbonates. Figure 5C demonstrates that $n_F/(n_F + n_{OH}) > 0.55$ in grandites from metacarbonate. Although there is evidence to suggest that Yun's analyses may be in error, the data in Figure 5C show that $n_F > n_{OH}$ in all available analyses of fluorian grandite from metacarbonates. The two Adirondack garnet analyses given by Valley et al. (1983) suggest a wide range in $n_F/(n_F + n_{OH})$ from this locality; however, $n_F/(n_F + n_{OH})$ from the two skarn localities is near 1.0. In contrast to the garnets from metacarbonates, $n_F/(n_F + n_{OH})$ in those from alkaline rocks and metabasalts is <0.50, suggesting higher OH contents of garnets formed in these lithologies. If it is not an artifact of the charge-balance calculation, the difference between calculated OH in metacarbonate garnets and that in garnets from the other localities may suggest that garnet compositions record contrasts in fluid composition between the environments. For example, the lower OH garnets from metacarbonates may reflect lower H_2O activities in fluids coexisting with metacarbonates. However, direct determination of H_2O content using IR spectroscopy combined with detailed petrology is required to resolve this relationship.

Fluorian calcic garnets and metamorphic fluid composition

Compositional relations between fluorian grandite and a coexisting fluid may be evaluated by consideration of the constraints imposed by heterogeneous equilibrium. Two linearly independent reactions in the system CaO-Al_2O_3-SiO_2-H_2O-HF describe the exchange of F, OH, and Si between real or hypothetical stoichiometric garnet end-members:

$$\underset{\text{grossular}}{Ca_3Al_2Si_3O_{12}} + 12H^+ + 12F^- = \underset{\text{F-grossular}}{Ca_3Al_2\square_3F_{12}} + 3SiO_{2(aq)} + 6H_2O \quad (4a)$$

and

$$\underset{\text{hydrogrossular}}{Ca_3Al_2\square_3(OH)_{12}} + 12H^+ + 12F^- = \underset{\text{F-grossular}}{Ca_3Al_2\square_3F_{12}} + 12H_2O. \quad (4b)$$

The mass-action relations for these equations are

$$\log K_{4a} = 3 \log a_{SiO_{2(aq)}} + 6 \log a_{H_2O} - 12 \log a_{H^+}a_{F^-} + \log \frac{a_{Ca_3Al_2\square_3F_{12}}}{a_{Ca_3Al_2Si_3O_{12}}} \quad (5a)$$

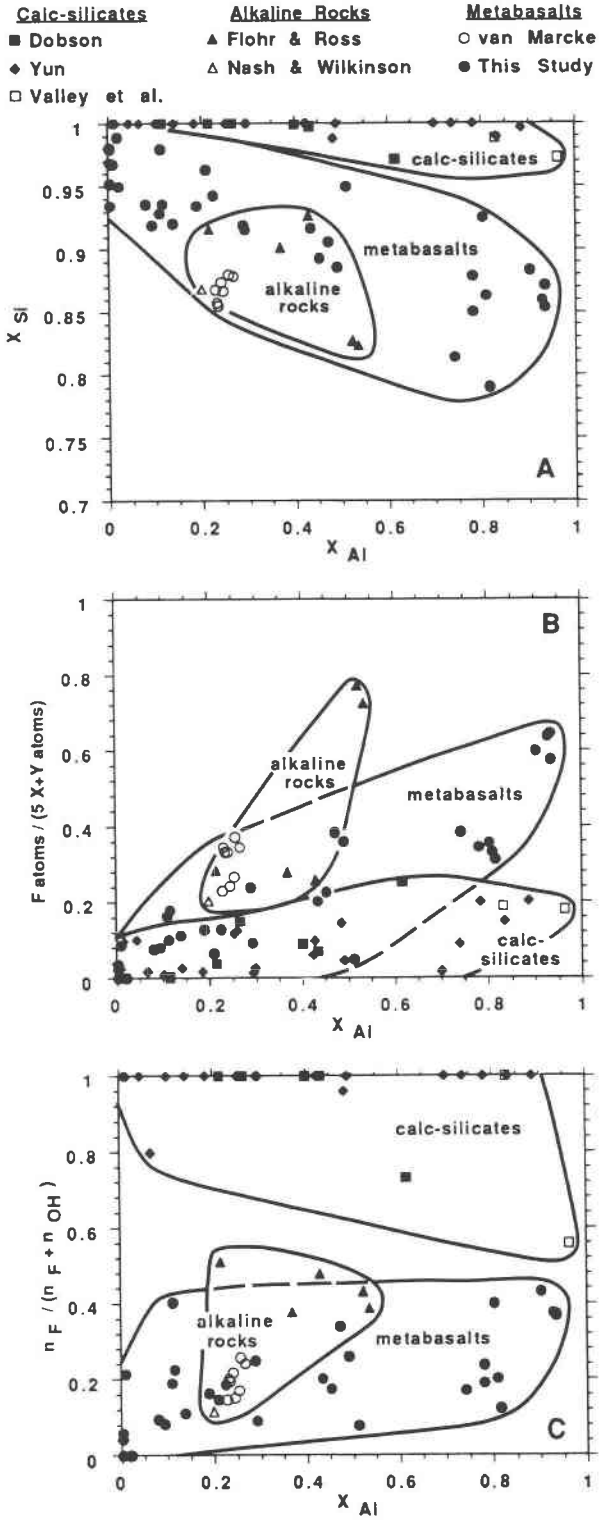

Fig. 5. Fluorian garnet compositions from alkaline igneous rocks, metacarbonates (mc) and metabasalts in terms of (**A**) mole fraction of Si, (**B**) F atoms per 5 (X + Y) atoms, and (**C**) $n_F/(n_F + n_{OH})$, all vs. mole fraction of Al. Solid lines represent compositional limits of garnets from each environment.

and

$$\log K_{4b} = 12 \log a_{H_2O} - 12 \log a_{H^+}a_{F^-} + \log \frac{a_{Ca_3Al_2\square_3F_{12}}}{a_{Ca_3Al_2\square_3(OH)_{12}}}, \quad (5b)$$

where a is activity and K is the equilibrium constant of the subscripted reaction. Standard-state conventions adopted in this study include unit activity of pure solids and H_2O at any pressure and temperature, unit activity of aqueous species other than H_2O in a hypothetical, 1 molal solution referenced to infinite dilution at any pressure and temperature, and unit fugacity of gases at 1 bar and any temperature.

Assuming local equilibrium between garnet and fluid, variations in the activities of end-members in the garnet solid solution require systematic changes in the activities of H^+, F^-, $SiO_{2(aq)}$, and H_2O in the fluid phase. The relative magnitudes of these changes can be illustrated by differentiating Equations 5a and 5b with respect to the reaction progress variable (ξ; Helgeson, 1979) at constant temperature and pressure:

$$3\left[\frac{\partial \log \frac{(a_{H^+}a_{F^-})^4}{a^2_{H_2O}a_{SiO_{2(aq)}}}}{\partial \xi_{4a}}\right]_{P,T} = \left[\frac{\partial \log \frac{a_{Ca_3Al_2\square_3F_{12}}}{a_{Ca_3Al_2Si_3O_{12}}}}{\partial \xi_{4a}}\right]_{P,T} \quad (6a)$$

and

$$12\left[\frac{\partial \log \frac{a_{H^+}a_{F^-}}{a_{H_2O}}}{\partial \xi_{4b}}\right]_{P,T} = \left[\frac{\partial \log \frac{a_{Ca_3Al_2\square_3F_{12}}}{a_{Ca_3Al_2\square_3(OH)_{12}}}}{\partial \xi_{4b}}\right]_{P,T} \quad (6b)$$

Equation 6b states that changes in $\log(a_{H^+}a_{F^-}/a_{H_2O})$ in the fluid phase are proportional to changes in $\log(a_{Ca_3Al_2\square_3F_{12}}/a_{Ca_3Al_2\square_3(OH)_{12}})$ by a factor of 12. Similarly, Equation 6a shows that changes in $\log(a_{Ca_3Al_2\square_3F_{12}}/a_{Ca_3Al_2Si_3O_{12}})$ are related to changes in $a_{H^+}a_{F^-}$, $a_{SiO_{2(aq)}}$, and a_{H_2O}, but in this case the proportionality is more complex due to the different stoichiometries of the aqueous species in Reaction 4a. Equation 6 also demonstrates that the activity ratios of garnet end-members are extremely sensitive to minor changes in fluid composition. For example, under conditions of constant $a_{SiO_{2(aq)}}$, and a_{H_2O}, Equations 6a and 6b reduce to

$$12\left[\frac{\partial \log a_{H^+}a_{F^-}}{\partial \xi}\right]_{P,T} = \left[\frac{\partial \log \frac{a_{Ca_3Al_2\square_3F_{12}}}{a_{Ca_3Al_2\square_3(OH)_{12}}}}{\partial \xi}\right]_{P,T} = \left[\frac{\partial \log \frac{a_{Ca_3Al_2\square_3F_{12}}}{a_{Ca_3Al_2Si_3O_{12}}}}{\partial \xi}\right]_{P,T}, \quad (7)$$

indicating that garnet compositions depend on F concentration and pH in the fluid to the extent that a change of $\log a_{H^+}a_{F^-}$ of 0.1 leads to a change in the activity ratio for garnet end-members of 1.2 log units.

The chemical potential (μ) of the thermodynamic component HF can be expressed as

$$\mu_{HF} = \mu^\circ_{HF} + RT \ln a_{HF}. \quad (8)$$

In Equations 4–7 we use the aqueous species H^+ and F^- to define μ_{HF} because pH is a useful geochemical variable for describing metasomatic processes and mineral hydrolysis. It is important to note, however, that alternate species such as $HF_{(aq)}$, $HF_{(gas)}$, or $H_{2(gas)}$ and $F_{2(gas)}$ could also be used. This can be seen by writing the following reactions between the thermodynamic component HF and these species:

$$HF = H^+ + F^-, \quad (9a)$$
$$HF = HF_{(aq)}, \quad (9b)$$
$$HF = HF_{(gas)}, \quad (9c)$$

and

$$2HF = H_{2(gas)} + F_{2(gas)}. \quad (9d)$$

Differentiating Equation 8 and the mass-action expressions for Equations 9a–d with respect to ξ yields

$$\frac{1}{2.3RT}\left[\frac{\partial \mu_{HF}}{\partial \xi}\right]_{P,T} = \left[\frac{\partial \log a_{H^+}a_{F^-}}{\partial \xi}\right]_{P,T} = \left[\frac{\partial \log a_{HF_{(aq)}}}{\partial \xi}\right]_{P,T} = \left[\frac{\partial \log f_{HF_{(gas)}}}{\partial \xi}\right]_{P,T} = \frac{1}{2}\left[\frac{\partial \log f_{H_{2(gas)}}f_{F_{2(gas)}}}{\partial \xi}\right]_{P,T} \quad (10)$$

(Helgeson, 1970), where f denotes fugacity of the subscripted gas. These relations demonstrate that changes in the activity or fugacity of each species can be equated to changes in μ_{HF} in precisely the same way.

Finally, Equations 7 and 10 can be combined to give

$$\frac{5.2}{RT}\left[\frac{\partial \mu_{HF}}{\partial \xi}\right]_{P,T} = \left[\frac{\partial \log \frac{a_{Ca_3Al_2\square_3F_{12}}}{a_{Ca_3Al_2\square_3(OH)_{12}}}}{\partial \xi}\right]_{P,T} = \left[\frac{\partial \log \frac{a_{Ca_3Al_2\square_3F_{12}}}{a_{Ca_3Al_2Si_3O_{12}}}}{\partial \xi}\right]_{P,T}. \quad (11)$$

Equation 11 shows that changes in the composition of fluorian hydrous grandite explicitly define changes in μ_{HF}. Similar relations may be written to illustrate that variations in garnet compositions also define changes in the chemical potentials of the thermodynamic components SiO_2 and H_2O.

Mineral-fluid equilibria involving East Greenland fluorian garnet

The value of $a_{H^+}a_{F^-}$ in the fluid in local equilibrium with fluorian grandites from East Greenland can be determined using phase relations and fluid inclusion observations. This value can then be combined with Equations 5 and 6 to examine how variations in $a_{H^+}a_{F^-}$ in the fluid are reflected in measured changes in the F content of garnet. Phase relations are presented below using equations and data of Helgeson et al. (1978, 1981).

Fluorian calcic garnets in the East Greenland metabasalts coexist with wollastonite (>99 mol% $CaSiO_3$) and stoichiometric fluorite and quartz. Equilibrium among these minerals and an aqueous solution can be represented by the reaction

$$\underset{\text{wollastonite}}{CaSiO_3} + 2H^+ + 2F^- = \underset{\text{fluorite}}{CaF_2} + \underset{\text{quartz}}{SiO_2} + H_2O \quad (12)$$

for which

$$\log K_{12} = \log \frac{a_{CaF_2} a_{SiO_2} a_{H_2O}}{a_{CaSiO_3} a_{H^+}^2 a_{F^-}^2}. \quad (13)$$

The isobaric temperature dependence of log K_{12} is given at various pressures in Figure 6. At ≤500 bars the large variations in the electrostatic properties and density of H_2O lead to a change from small negative to large positive values of the standard molal enthalpy of Reaction 12 (ΔH°_{12}) and result in extreme pressure and temperature dependence of log K_{12}. In contrast, the relatively small change in ΔH°_{12} with temperature at ≥1 kbar results in only slight variations in log K_{12} over the temperature of garnet formation. The change in log K_{12} illustrated in Figure 6, which is larger with isothermal pressure variation than with isobaric temperature change at ≥1 kbar, indicates that accurate knowledge of the pressure is important for evaluation of phase relations involving Reaction 12. As noted above, stratigraphic reconstructions indicate a lithostatic pressure of 1 kbar for garnet formation (Manning, 1989). At this pressure, a minimum in log K_{12} occurs at 311 °C, reflecting the fact that $\Delta H^\circ_{12} = 0$ at this temperature and the relatively small temperature dependence of log K_{12} at this pressure (Fig. 6) is a consequence of the small magnitude of the change in the standard-state heat capacity of Reaction 12 at 1 kbar. In the calculations presented below we assumed the temperature of garnet formation was 350 °C. For 350 °C, 1 kbar, and pure solids, Equation 13 reduces to

$$\log a_{H^+}a_{F^-} - \tfrac{1}{2} \log a_{H_2O} = -10.06, \quad (14)$$

where −10.06 is −0.5 log K_{12}. Although we have fixed temperature at 350 °C, it should be emphasized that the right side of Equation 14 varies by only −0.5 log units over the possible temperature range of garnet formation; for example, this quantity is −10.42 at 200 °C, −10.00 at 311 °C, and −10.50 at 420 °C (Fig. 6).

Equation 14 indicates that determination of log $a_{H^+}a_{F^-}$ in a fluid in equilibrium with fluorian garnet, wollastonite, fluorite, and quartz requires knowledged of the activity of H_2O. The value of a_{H_2O} associated with garnet formation can be constrained using salinities of quartz fluid inclusions in a granophyre vein near sample 844O (Fig. 2), which are ~8 wt% NaCl equivalent, 1.5 molal (Bird et al., 1986). If fluorian garnet formation were associated with mixing of these fluids with dilute pore solutions as we suggested above, the total salinities would be lower than 8 wt%. Nevertheless, the lowest possible H_2O activity can be determined by assuming this value. At <400 °C and 1 kbar, the presence of calcite in the retrograde alteration assemblage requires this minimum value of a_{H_2O} to have been 0.97 as constrained by the reaction

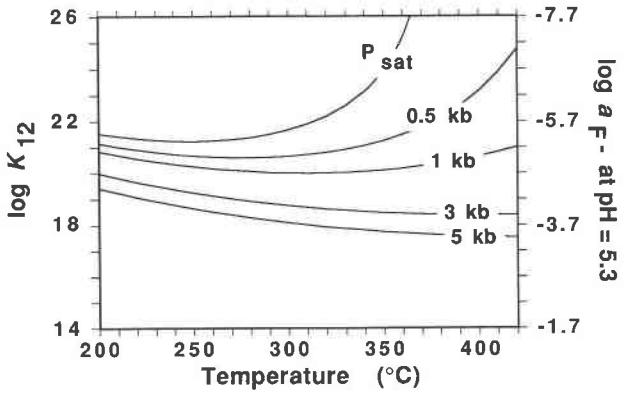

Fig. 6. Logarithm of the equilibrium constant for Reaction 12 (log K_{12}; see text) as a function of temperature. The isopleths represent isobaric values of log K_{12} at the designated pressure, with the exception of the P_{sat} isopleth, along which pressures correspond to liquid-vapor equilibrium for pure H_2O. Values for log K_{12} were calculated using the data of Helgeson et al. (1978, 1981). The right vertical axis shows values of log a_{F^-} at pH = 5.3 (see text).

$$\underset{\text{wollastonite}}{CaSiO_3} + CO_2 = \underset{\text{calcite}}{CaCO_3} + \underset{\text{quartz}}{SiO_2} \quad (15)$$

using the equations and data of Bowers and Helgeson (1983). If 8 wt% NaCl equivalent were assumed, the value of log $a_{H^+}a_{F^-}$ in the fluid coexisting with fluorian grandite garnets would have been −10.07 at 350 °C and 1 kbar (Eq. 14); but if a_{H_2O} were unity, log $a_{H^+}a_{F^-}$ would have been −10.06. This demonstrates that a_{H_2O} has little effect on the present calculations, and we have assumed that $a_{H_2O} = 1.0$.

At $a_{H_2O} = 1$, log a_{F^-} associated with garnet formation is linearly dependent on pH (Eq. 14). The right vertical axis in Figure 6 gives values of log a_{F^-} for pH = 5.3, which corresponds to neutral pH (±0.1) of pure H_2O at 1 kbar and 200–420 °C. Figure 6 thus shows that if pH were neutral, log a_{F^-} associated with fluorian garnet formation near the Skaergaard intrusion would have been between −4.7 and −5.2.

Figure 7A shows stoichiometric mineral stabilities as a

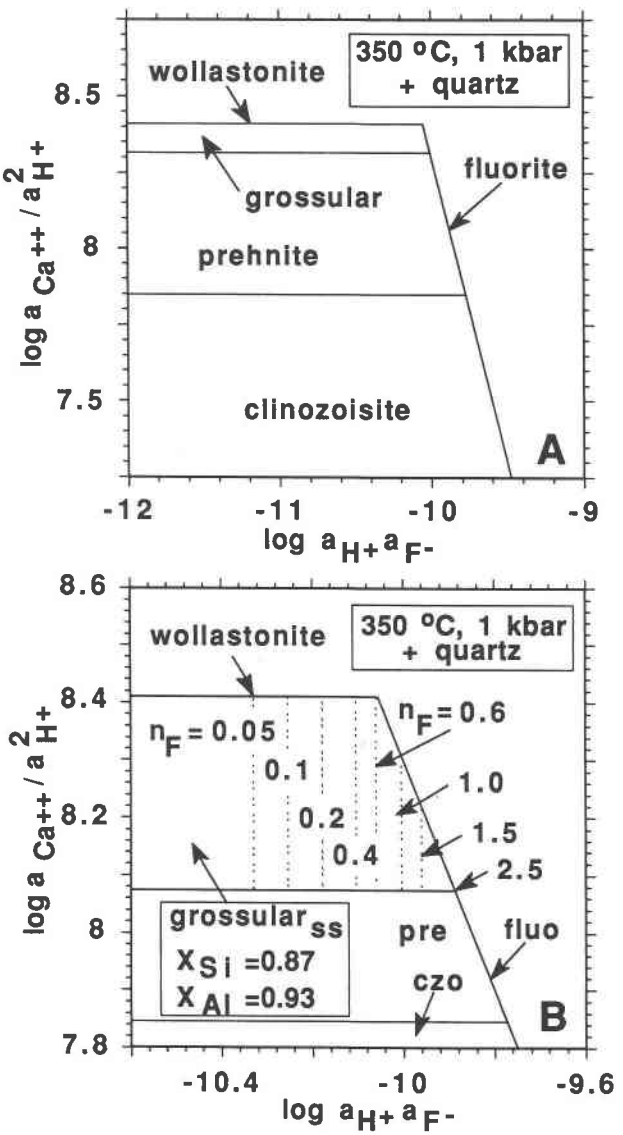

Fig. 7. (**A**) Stoichiometric phase relations in the system CaO-Al_2O_3-SiO_2-H_2O-HF at 350 °C and 1 kbar in equilibrium with quartz and pure H_2O in terms of log $a_{Ca^{2+}}/a^2_{H^+}$ and log $a_{H^+}a_{F^-}$. (**B**) Phase relations involving silica-deficient, hydrous, fluorian grossular at 350 °C and 1 kbar in equilibrium with quartz and pure H_2O in terms of log $a_{Ca^{2+}}/a^2_{H^+}$ and log $a_{H^+}a_{F^-}$. The dashed vertical lines denote the number of F atoms per 5 (X + Y) atoms required by Reaction 4a (see text).

function of log $a_{Ca^{2+}}/a^2_{H^+}$ and log $a_{H^+}a_{F^-}$ in the fluid phase in equilibrium with quartz and pure H_2O at 350 °C and 1 kbar in the system CaO-Al_2O_3-SiO_2-H_2O-HF. The wollastonite and fluorite phase boundaries represent fluid saturation limits in this projection and define maximum values of log $a_{Ca^{2+}}/a^2_{H^+}$ and log $a_{H^+}a_{F^-}$ that may be attained in the fluid without supersaturation of either phase. The phase relations illustrated in Figure 7A indicate that at progressively higher log $a_{Ca^{2+}}/a^2_{H^+}$ in the coexisting fluid, the successively stable phases are clinozoisite, prehnite, and grossular, and that the maximum log $a_{Ca^{2+}}/a^2_{H^+}$ occurs in equilibrium with grossular and wollastonite. The minimum value of log $a_{H^+}a_{F^-}$ for fluorite saturation is −10.06, corresponding to equilibrium among wollastonite, fluorite, and quartz. The negative slope of the fluorite saturation surface indicates that, with decreasing log $a_{Ca^{2+}}/a^2_{H^+}$, higher values of log $a_{H^+}a_{F^-}$ are required to maintain equilibrium between fluorite and the fluid phase. Figure 7A also shows that the conditions inferred for the formation of the East Greenland garnets in amygdule centers correspond to the intersection of the wollastonite and fluorite saturation surfaces log $a_{Ca^{2+}}/a^2_{H^+} \leq 8.13$, indicating a gradient in log $a_{Ca^{2+}}/a^2_{H^+}$ from amygdule margins to amygdule centers of at least 0.28 log units over distances of several millimeters.

The variation in log $a_{H^+}a_{F^-}$ in the fluid as a function of the extent of F and OH substitution in garnet can be predicted using Equation 5 with measured East Greenland garnet compositions. In the absence of experimental constraints on the effects of F and OH substitution in grandite, we have adopted an ideal ionic mixing approximation such that $a_{Ca_3Al_2Si_3O_{12}} = X^2_{Al}X^2_{Si}$, $a_{Ca_3Al_2\square_3F_{12}} = X^2_{Al}(n_F/12)^3$, and $a_{Ca_3Al_2\square_3(OH)_{12}} = X^2_{Al}(n_{OH}/12)^3$. Because there is evidence for nonideal mixing along the grossular-andradite join (e.g., Engi and Wersin, 1987), we evaluated phase relations for Al-rich garnets to minimize the effect of possible deviations from ideality.

Taking a_{H_2O} as unity and substituting quartz for $SiO_{2(aq)}$ in Reactions 4a and 4b as required by the presence of this phase in the alteration assemblage, Equations 5a and 5b can be written as

$$\log K_{4a} = -12 \log a_{H^+}a_{F^-} + 3 \log \frac{n_F/12}{X_{Si}} \quad (16a)$$

and

$$\log K_{4b} = -12 \log a_{H^+}a_{F^-} + 3 \log \frac{n_F}{n_{OH}}. \quad (16b)$$

Figure 4B shows that X_{Si} varies widely in the grossular-rich ($X_{Al} > 0.75$) garnets of this study. Taking the average values of $X_{Si} = 0.87$ and $X_{Al} = 0.93$ for the most Al-rich group of analyses from sample 1187 (Fig. 4B), the value of $a_{Ca_3Al_2Si_3O_{12}}$ in the garnets is 0.57. Similarly, the most Al-rich garnets have $n_F = 0.6$ (Fig. 4A) and $n_{OH} = 1.0$, yielding values of $a_{Ca_3Al_2\square_3F_{12}}$ and $a_{Ca_3Al_2\square_3(OH)_{12}}$ equal to 1.1×10^{-4} and 5.0×10^{-4}, respectively. When combined with Equations 14 and 16, these activities yield values for log K_{4a} equal to 117.0 and log K_{4b} equal to 120.1 in the presence of quartz, wollastonite, fluorite, and pure H_2O. Equations 16a and 16b may now be rewritten as

$$\log a_{H^+}a_{F^-} = 0.25 \log \frac{(n_F/12)}{X_{Si}} - 9.75, \quad (17a)$$

and

$$\log a_{H^+}a_{F^-} = 0.25 \log \frac{n_F}{n_{OH}} - 10.01, \quad (17b)$$

showing that in the absence of mineral assemblages such as wollastonite + fluorite + quartz, fluorian grandite compositions can be used to determine $a_{H^+}a_{F^-}$ in aqueous solutions. In principle, either Equation 17a or 17b will give the same value of log $a_{H^+}a_{F^-}$; however in practice, the large uncertainties in calculated OH from electron microprobe analyses lead to large uncertainties in solutions to Equation 17b. Thus Equation 17a should be used to determine $a_{H^+}a_{F^-}$ in the fluid in the absence of a direct OH determination.

The isothermal, isobaric relations between log $a_{H^+}a_{F^-}$ and garnet composition as computed from Equation 17a are in Figure 7B in terms of F atoms per 5 (X + Y) atoms. Figure 7B illustrates that the F content of grossular solid solution increases with increasing $a_{H^+}a_{F^-}$ in the coexisting fluid phase. For values of log $a_{H^+}a_{F^-}$ less than -10.40 in the fluid phase, F in the coexisting garnet will be below electron microprobe detection limit [<0.027 atoms per 5 (X + Y) atoms] using the analytical conditions employed in this study. In the presence of fluorite and quartz, the F concentration in garnet increases with decreasing log $a_{Ca^{2+}}/a^2_{H^+}$. Figure 7B shows that the maximum F content in garnet at 350 °C and 1 kbar ($n_F \sim 2.5$) will be attained in the presence of prehnite, fluorite, and quartz. The extreme sensitivity of garnet chemistry to fluid composition can be seen in Figure 7B by noting that increasing the value of n_F in garnet from <0.05 to 0.60 requires a change in either pH or log a_{F^-} of only 0.3. The relative topology of phase relations and n_F isopleths in Figure 7B are the same independent of the temperature range assumed for garnet formation. However, the values of log $a_{Ca^{2+}}/a^2_{H^+}$ and log $a_{H^+}a_{F^-}$ for phase boundaries and n_F isopleths will change with temperature: if the garnets formed at 200 °C, the intersection of the wollastonite and fluorite saturation surfaces and the $n_F = 0.6$ isopleth will occur at log $a_{Ca^{2+}}/a^2_{H^+} = 11.05$ and log $a_{H^+}a_{F^-} = -10.42$, whereas at 400 °C these values are, respectively, 7.68 and -10.32.

Mineral-fluid equilibria in Adirondack calc-silicates

The amount of F and values of $n_F/(n_F + n_{OH})$ vary among different geologic environments (Fig. 5), suggesting that the garnets record differences in metamorphic fluid composition at each locality. Unfortunately, the pressures and temperatures of formation of most fluorian garnets are either highly uncertain or are not reported. In view of the possible effects of pressure and temperature on such comparisons (Fig. 6), a detailed understanding of how variations in garnet composition depend on temperature and pressure will only be possible when more F-bearing garnet occurrences are described. However, the utility of using fluorian garnet phase relations to compare metamorphic fluid compositions can be illustrated by assuming isothermal and isobaric conditions among different localities. As an example, we compare fluid compositions in the East Greenland garnet occurrence with those associated with fluorian garnets in the Adirondacks, for which the associated mineral assemblage is well documented.

Aluminum-rich, fluorian calcic garnets associated with retrograde alteration of Adirondack calc-silicates have lower F concentrations and higher $n_F/(n_F + n_{OH})$ relative to garnets of the metabasalts into which the Skaergaard intrudes (Fig. 5C). Simultaneous consideration of Equations 5a and 5b suggests lower values of both a_{H_2O} and $a_{H^+}a_{F^-}$ in the fluid associated with the Adirondack garnets relative to those near the Skaergaard intrusion. The values of log $a_{H^+}a_{F^-}$ in Adirondack calc-silicates can be estimated with garnet compositions by first constraining a_{H_2O} from phase relations among coexisting minerals, which include prehnite, calcite, pumpellyite, and quartz but not fluorite (Valley et al., 1983). The most Al-rich garnet reported by Valley et al. (1983) has $n_F = 0.18$, $X_{Si} = 0.97$, and $X_{Al} = 0.96$. These values result in activities of $Ca_3Al_2Si_3O_{12}$ and $Ca_3Al_2\square_3F_{12}$ of 0.84 and 0.34×10^{-5}, respectively, using the above approximations of activity. If the fluid were a mixture of H_2O and CO_2, the intersection of the equilibrium

$$\underset{\text{prehnite}}{Ca_2Al_2Si_3O_{10}(OH)_2} + \underset{\text{calcite}}{CaCO_3} = \underset{\text{grossular}}{Ca_3Al_2Si_3O_{12}} + H_2O + CO_2 \qquad (18)$$

with the reaction defining the maximum stability of prehnite,

$$5\underset{\text{prehnite}}{Ca_2Al_2Si_3O_{10}(OH)_2} = 2\underset{\text{grossular}}{Ca_3Al_2Si_3O_{12}} + 3\underset{\text{quartz}}{SiO_2} + 2\underset{\text{zoisite}}{Ca_2Al_3Si_3O_{12}(OH)} + 4h_2O, \qquad (19)$$

would require a maximum X_{CO_2} of 0.01 and a minimum a_{H_2O} of 0.99 at 350 °C and 1 kbar, if one uses the equations and data of Helgeson et al. (1978) and Bowers and Helgeson (1983). This leads to log $a_{H^+}a_{F^-} = -10.21$ from solution of Equation 5A at quartz saturation. Increasing a_{H_2O} to 1.0 results in log $a_{H^+}a_{F^-} = -10.20$, showing that this calculation is also relatively insensitive to the water activity adopted. Thus, if the Adirondack garnets were to have formed at 350 °C and 1 kbar, values of log $a_{H^+}a_{F^-}$ 0.14–0.15 log units more negative than those associated with the East Greenland garnets would indicate a lower μ_{HF} (Eq. 10) in the coexisting fluid phase in the former locality.

Conclusions

The F content of hydrous grandite garnets in the basaltic host rocks of the Skaergaard intrusion increases with increasing X_{Al} and calculated OH and decreasing X_{Si}. Similar trends are exhibited by F-bearing garnets in metasomatically altered alkaline igneous rocks and metamorphosed carbonates. Values of $n_F/(n_F + n_{OH})$ also increase with increasing X_{Al}. Compositions of fluorian garnets from East Greenland indicate that F substitutes with OH to compensate silica deficiency.

The distribution of garnet compositions in the Skaergaard host basalts is consistent with formation at 200–420 °C, as constrained by the coexisting mineral assemblage. Phase relations in the Skaergaard host basalts show that log $a_{H^+}a_{F^-}$ in the coexisting fluid phase was between −10.0 and −10.5 at 1 kbar and 200–420 °C. If pH were neutral, log a_{F^-} associated with the formation of the F-bearing garnets of this study would have been −4.7 to −5.2. The calculations presented here predict that fluorian garnet compositions are extremely sensitive to changes in pH or the activity of F^- in the fluid phase. If pressures and temperatures were similar, phase equilibrium constraints indicate that lower n_F and higher $n_F/(n_F + n_{OH})$ in garnets from Adirondack calc-silicates relative to those from East Greenland reflect lower log $a_{H^+}a_{F^-}$ of −10.21. These results show that F content of garnet associated with low-temperature alteration can provide an excellent basis for evaluating activities of F species in coexisting metamorphic fluids.

Acknowledgments

This paper represents a portion of the senior author's Ph.D. dissertation at Stanford University. We thank Jim Munoz and John Valley, whose insightful reviews improved the manuscript. The comments of Nick Rose, J.G. Liou, Eric Seedorff, and Lou Caruso on early versions of this work are gratefully acknowledged. Financial support for this study was provided by the Geological Society of America, a Corning Glass Science Fellowship, and NSF grants 84-18129, 86-06256, and 88-03754 to D.K. Bird and 86-15714 to S.R. Bohlen. Field research was aided by the logistical support of Platinova Resources, Ltd., and the Greenland Geological Survey. We also thank Minik Rosing, Kent Brooks, and Troels Nielsen for their advice and help.

References cited

Barton, M.D., Haselton, H.J., Hemingway, B.S., Kleppa, O.J., and Robie, R.A. (1982) The thermodynamic properties of fluor-topaz. American Mineralogist, 67, 350–355.

Bence, A.E., and Albee, A.L. (1968) Empirical correction factors for the electron microanalysis of silicates and oxides. Journal of Geology, 76, 382–403.

Bird, D.K., and Helgeson, H.C. (1980) Chemical interaction of aqueous solutions with epidote-feldspar mineral assemblages in geologic systems. I. Thermodynamic analysis of phase relations in the system CaO-FeO-Fe_2O_3-Al_2O_3-SiO_2-H_2O-CO_2. American Journal of Science, 280, 907–941.

Bird, D.K., Rogers, R.D., and Manning, C.E. (1986) Mineralized fracture systems of the Skaergaard intrusion. Meddelelser om Grønland, Geoscience, 16, 68 p.

Bird, D.K., Manning, C.E., and Rose, N.M. (1988a) Hydrothermal alteration of Tertiary layered gabbros, East Greenland. American Journal of Science, 288, 405–457.

——— (1988b) Mineralogic and isotopic constraints on the regional hydrology of the Skaergaard magma-hydrothermal system, East Greenland. Geological Society of America Abstracts with Programs, 20 (7), A344–A345.

Bird, D.K., Rosing, M.T., Manning, C.E., and Rose, N.M. (1985) Geologic field studies of the Miki Fjord area, East Greenland. Geological Society of Denmark Bulletin, 34, 219–236.

Bowers, T.S., and Helgeson, H.C. (1983) Calculation of the thermodynamic and geochemical consequences of nonideal mixing in the system H_2O-CO_2-NaCl on phase relations in geologic systems: Equation of state for H_2O-CO_2-NaCl fluids at high pressures and temperatures. Geochimica et Cosmochimica Acta, 47, 1247–1275.

Chambers, W.F. (1985) SANDIA TASK8: a subroutined electron microprobe automation system. Sandia National Laboratories Report SAND85-2037, 115 p.

Cohen-Addad, P.C., Ducros, P., and Bertant, E.F. (1967) Étude de la substitution du groupement SiO_4 par $(OH)_4$ dans les composés $Al_2Ca_3(OH)_{12}$ et $Al_2Ca_3(SiO_4)_{2.16}(OH)_{3.36}$ de type grenat. Act Crystallographica, 23, 220–330.

Connolly, J.A.D., and Kerrick, D.M. (1985) Experimental and thermodynamic analysis of prehnite stability (abs.). EOS, 66, 388.

Deer, W.A., Howie, R.A., and Zussman, J. (1982) Rock-Forming Minerals, vol. 1A: Orthosilicates (second edition), 919 p. Wiley, New York.

Dobson, D.C. (1982) Geology and alteration of the Lost River tin-tungsten-fluorine deposit, Alaska. Economic Geology, 77, 1033–1052.

——— (1984) Geology and geochemical evolution of the Lost River, Alaska, tin deposit. Ph.D. thesis, Stanford University, Stanford, California.

Engi, M., and Wersin, P. (1987) Derivation and application of a solution model for calcic garnet. Schweizerische Mineralogische und Petrographische Mitteilungen, 67, 53–73.

Eugster, H.P., and Wones, D.R. (1962) Stability relations of the ferruginous biotite, annite. Journal of Petrology, 3, 82–125.

Flohr, M.J.K., and Ross, M. (1989) Alkaline igneous rocks of Magnet Cove, Arkansas: Metasomatized ijolite xenoliths from Diamond Jo quarry. American Mineralogist, 74, 113–131.

Gustafson, W.I. (1974) The stability of andradite, hedenbergite, and related minerals in the system Ca-Fe-Si-O-H. Journal of Petrology, 15, 455–496.

Helgeson, H.C. (1970) Description and interpretation of phase relations in geochemical processes involving aqueous solutions. American Journal of Science, 268, 415–438.

Helgeson, H.C. (1979) Mass transfer among minerals and hydrothermal solutions. In H.L. Barnes, Ed., Geochemistry of hydrothermal ore deposits (second edition), p. 568–610. Wiley, New York.

Helgeson, H.C., Delany, J.M., Nesbitt, H.W., and Bird, D.K. (1978) Summary and critique of the thermodynamic properties of rock-forming minerals. American Journal of Science, 278-A, 229 p.

Helgeson, H.C., Kirkham, D.H., and Flowers, G.C. (1981) Theoretical prediction of the thermodynamic behavior of aqueous electrolytes at high pressures and temperatures: IV. Calculation of activity coefficients, osmotic coefficients, and apparent molal and standard and relative partial molal properties to 600 °C and 5 KB. American Journal of Science, 281, 1249–1516.

Huckenholz, H.G., and Fehr, K.T. (1982) Stability relationships of grossular + quartz + wollastonite + anorthite: II. The effects of grandite-hydrograndite solid solution. Neues Jahrbuch für Mineralogie Abhandlungen, 145, 1–33.

Huggins, F.E., Virgo, D., and Huckenholz, H.G. (1977) Titanium-containing silicate garnets. II. The crystal chemistry of melanites and schorlomites. American Mineralogist, 62, 646–665.

Korzhinskii, M.A. (1981) Apatite solid solutions as indicators of the fugacity of HCl and HF in hydrothermal fluids. Geochemistry International, 18(3), 44–60.

Lager, G.A., Ambruster, T., and Faber, J. (1987) Neutron and X-ray diffraction study of hydrogarnet $Ca_3Al_2(O_4H_4)_3$. American Mineralogist, 72, 758–767.

Lager, G.A., Ambruster, T., Rotella, F.J., and Rossman, G.R. (1989) OH substitution in garnets: X-ray and neutron diffraction, infrared, and geometric-modeling studies. American Mineralogist, 74, 840–851.

Liou, J.G. (1971) Synthesis and stability relations of prehnite, $Ca_2Al_2Si_3O_{10}(OH)$. American Mineralogist, 56, 507–531.

Manning, C.E. (1989) Porosity evolution, contact metamorphism, and fluid flow in the host basalts of the Skaergaard magma-hydrothermal system. Ph.D. thesis, Stanford University, Stanford, California.

Manning, C.E., and Bird, D.K. (1986) Hydrothermal clinopyroxenes of the Skaergaard intrusion. Contributions to Mineralogy and Petrology, 92, 437–447.

Meagher, E.P. (1980) Silicate garnets. Mineralogical Society of America Reviews in Mineralogy, 5, 25–66.

Munoz, J.L. (1984) F-OH and Cl-OH exchange in micas with applications to hydrothermal ore deposits. Mineralogical Society of America Reviews in Mineralogy, 13, 469–493.

Munoz, J.L., and Ludington, S.D. (1974) Fluorine-hydroxyl exchange in biotite. American Journal of Science, 274, 396–413.

——— (1977) Fluoride-hydroxyl exchange in synthetic muscovite and its application to muscovite-biotite assemblages. American Mineralogist, 62, 304–308.

Nash, W.P., and Wilkinson, J.F.G. (1970) Shonkin sag laccolith, Montana. I. Mafic minerals and estimates of temperature, pressure, oxygen fugacity and silica activity. Contributions to Mineralogy and Petrology, 25, 241–269.

Norton, D., and Taylor, H.P., Jr. (1979) Quantitative simulation of the hydrothermal systems of crystallizing magmas on the basis of transport theory and oxygen isotope data: an analysis of the Skaergaard intrusion. Journal of Petrology, 20, 421–486.

Norton, D., Taylor, H.P., Jr., and Bird, D.K. (1984) The geometry and high temperature brittle deformation of the Skaergaard intrusion. Journal of Geophysical Research, 89, 10178–10192.

Pabst, A. (1942) Reexamination of hibschite. American Mineralogist, 27, 783–789.

Peters, T. (1965) A water-bearing andradite from Totalp serpentine (Davos, Switzerland). American Mineralogist, 50, 1482–1486.

Rose, N.M., and Bird, D.K. (1987) Prehnite-epidote phase relations in the Nordre Aputitêq and Kruuse Fjord layered gabbros, East Greenland. Journal of Petrology, 28, 1193–1218.

Seedorff, C.E. (1987) Henderson porphyry molybdenum deposit: cyclic alteration-mineralization and geochemical evolution of topaz- and magnetite-bearing assemblages. Ph.D. thesis, Stanford University, Stanford, California.

Smyth, J.R., Madel, R.E., McCormick, T.C., Munoz, J.L., and Rossman, G.R. (1990) Crystal-structure refinement of a F-bearing spessartine garnet. American Mineralogist, 75, 314–318.

Solberg, T.N. (1982) Fluorine electron microprobe analysis: variation of X-ray peak shape. In K.F.J. Heirich, Ed., Microbeam analysis—1982, p. 148–150, San Francisco Press, San Francisco.

Taylor, H.P., Jr., and Forester, R.W. (1979) An oxygen isotope study of the Skaergaard intrusion and its country rocks: a description of a 55-m.y. old fossil hydrothermal system. Journal of Petrology, 20, 355–419.

Valley, J.W., Essene, E.J., and Peacor, D.R. (1983) Fluorine-bearing garnets in Adirondack calc-silicates. American Mineralogist, 68, 444–448.

van Marcke de Lummen, G. (1986) Fluor-bearing hydro-andradite from an altered basalt in the Land's End area, SW England. Bulletin de Minéralogie, 109, 613–616.

van Marcke de Lummen, G., and Verkaeren, J. (1985) Mineralogical observations and genetic considerations relating to skarn formation at Botallack, Cornwall, England. In High heat production granites, hydrothermal circulation and ore genesis, p. 535–547. The Institution of Mining and Metallurgy, London.

Wager, L.R., and Deer, W.A. (1939) Geological investigations in East Greenland, Pt. III. The petrology of the Skaergaard intrusion, Kangerdlugssuak region. Meddelelser om Grønland, 134, 352 p.

Yun, S. (1979) Geology and skarn ore mineralization of the Yeonhwa-Ulchin zinc-lead mining district, southeastern Taebaegsan region, Korea. Ph.D. thesis, Stanford University, Stanford, California.

Yun, S., and Einaudi, M.T. (1982) Zinc-lead skarns of the Yeonhwa-Ulchin district, South Korea. Economic Geology, 77, 1013–1032.

Manuscript received July 7, 1989
Manuscript accepted April 16, 1990